Physical Education, Health and Social Sciences
https://journal-of-social-education.org
E-ISSN: 2958-5996
P-ISSN: 2958-5988

Wide-band Asymmetric Transmission for Linearly Polarized Wave Using Bi-layered Chiral Metamaterial

Engr Muhammad Asif Ramzan[1], Tariq Ullah[2], Dr. Shahzada Alamgir Khan[3], Muhammad Usama Awais[4]

[1,3] Dept. of Telecommunications, Institue of Communication Technology, University of Engineering & Technology Peshawar, asiframzan314@gmail.com, shahzada.alamgir@ptclgroup.com
[2] University of Engineering and Technology (UET), Taxila, tariqullah885@gmail.com
[4] Barani Institute of Sciences, Sahiwal, Email: usama.awais@baraniinstitute.edu.pk

DOI: https://doi.org/10.63163/jpehss.v3i2.264

Abstract

In this paper, a metal-dielectric-metal configuration is employed. The unit cell of the proposed chiral metamaterial design consists of a simple 'EI' shape resonator printed on two opposite sides of dielectric substrate. The metal pattern on the front and back layers is identical, with the exception that the back-layer pattern twisted at a 90^o angle to break mirror symmetry in the propagation direction. The optimized dimensions (in mm) of the unit cell are: w=1.5, w1=1.5, d=1, b=6, m=3, h=1.6 and a=8. The dielectric substrate is Roger 5080, which has a dielectric constant εr = 2.33, and tangent loss tan δ = 0.0005. The copper sheet is used as a metallic pattern having a thickness of 35um, and an electrical conductivity of 5.8 x 10^7 S/m. Commercially available software called CST Microwave Studio is used to carry out the numerical simulations of the suggested design. Unit-cell boundary conditions were applied in the y- and x-directions, while open boundary conditions were used in the z-direction. The numerical simulation is carried out in the frequency range of 11 GHz to 23 GHz. Through numerical simulation, complex transmission coefficients are produced, from which the asymmetric transmission, total transmission and polarization conversion ratio are calculated. The simulation results of complex transmission coefficients for linearly polarized waves in the forward (+z) and backward (-z) direction of propagation shows wide, strong peaks.

Keywords: Asymmetric Transmission, Chiral Metamaterial, Transmission coefficients, Linearly Polarized,

Introduction

The electromagnetic (EM) wave's polarization feature describes the direction and relative amplitude of the electric field vector at a fixed point in space as they change over time [1]. There are three different types of polarization: elliptical, circular, and linear modes. If the vector of the time-varying electric field at a particular location in space always oscillates along the same straight line, despite changes in magnitude, the wave is said to be linearly polarized. If the vector field (magnetic and electric) comprises a single component or two linearly polarized perpendicular components with a phase difference of either 0° or 180°, linear polarization is obtained. If the tip

of the electric vector at a certain location in space describes a circle around the propagation direction, the wave is said to be circularly polarized. A circularly polarized wave is equal to two linearly polarized waves of the same magnitude with an odd multiple of 90 degrees as their phase difference. Elliptically polarized wave occurs when the tip of the resulting electric field vector tracks an ellipse locus about the direction of propagation. Additionally, if a wave exhibits neither linear nor circular polarization, it is elliptically polarized. Moreover, if a wave exhibits neither linear nor circular polarization, it is said to be elliptically polarized. Periodically ordered artificial structures known as metamaterials exhibit intriguing EM features that are typically absent from nature. In 1968, Veselago [2] presented an unanticipated occurrence that is often expected in hypothetical left-handed materials, where a system of left-handed is formed by the set of three field vectors: magnetic (H), electric (E), and wave vector (k). Furthermore, he shows how the energy flow (pointing vector) of an electromagnetic wave is directed in relation to the wave vector or phase velocity. As a result, these substances are referred to as left-handed materials (LHM) [3]. Because of their simultaneous negative relative permeability and permittivity values, these materials are also known as negative index materials (NIM) [4-5]. The theoretical concept of negative relative permeability and permittivity was initially introduced by Veselago [2]. Pendry [6] examined a viable meta-structure that simultaneously yields a negative permittivity and permeability value. Afterwards, Smith used the resonant element structure in 2000 [7] to experimentally establish the negative permeability and permittivity of materials. By carefully planning the unit cell's shape and material, the metamaterial response may be precisely regulated. The unit cell may consist of a complicated structure that is two-dimensional (2-D) or three-dimensional (3-D), depending on the 2D [8–9] and 3D [10–12] metamaterials design. Effective medium theory (EMT) can be used to obtain the constitutive effective parameter (permittivity and permeability) of the metamaterial slab [13–17]. Due to its negative index of refraction, the left-handed metamaterial exhibits unusual electromagnetic features, such as perfect lensing or super-resolution [18–20], negative doppler effect [21], EM invisibility cloaking [22–27], negative refraction [28], and so on. In addition to these unique qualities, metamaterials find usage in applications such as polarization converters [29–31], electromagnetic absorbers [32–35], resonance magnetic imaging [36–37], antenna design [38–40], and sensors [41–43], where conventional materials were previously employed. Furthermore, it has been predicted that metamaterial-based structures will make possible a wide range of non-linear field applications, including non-linear mirror operation, second enhanced harmonic generation, non-linear magnetic and electric response, and backward phase matching [44–47]. Using an experimental method, non-linear active metamaterials are examined for the creation of solitons [48]. Metasurfaces are the 2D planar counterpart of bulk metamaterial [49–52]. The thickness of the metasurface is subwavelength, meaning that the wavelength of the impinging wave must be significantly larger than the overall thickness. The sheet impedance and boundary condition of metasurfaces are more descriptive than the effective constitutive parameter that characterized bulk metamaterials. Because of their three-dimensional complicated architecture, bulk metamaterials are difficult to produce at the micro- and nano-levels, making their practical applications limited. On the other hand, if a planar sheet is patterned in a periodic way, it can be easily transformed into a single [53–54] or multi-layer [55–59] design configuration. In comparison to bulk metamaterial, metasurface offers relatively less loss in the propagation direction because of its minuscule subwavelength thickness. Overall, metasurfaces—which strongly interact with electromagnetic waves to give a variety of potential functionalities—overcome the limitations of bulk metamaterials. Significant advancements have been made recently in the analytical formulation used for the metasurface's

design and analysis. A thorough examination of the analytical and numerical methods for the 2D and 3D metamaterials is provided in reference [60]. The more straightforward methods for creating and analyzing metasurfaces are the same as those used in electric circuit approximation, where the metasurface is defined by a particular combination of resistor, capacitor, and inductor, the optimal value of which is determined by the appropriate geometrical arrangement of the metasurface [61–64]. The EM wave's phase, intensity, and polarization state can be controlled and manipulated in both the transmitting and reflecting modes by designing a metasurface with the right unit cell geometry. From an application perspective, every mode of operation has a unique significance. The copper sheet is etched on the back of the metasurface during reflection mode operation to prevent wave transmission. On the other hand, no ground plane was needed for metasurface operation in transmission mode. The thorough analysis and an example of how the metamaterial is used in a reflection or transmission mode are covered in the next two sections. Chiral metamaterials (CMMs) are a novel family of metamaterials that can be used to control polarization conversion because they exhibit cross-coupling between the electric and magnetic fields at different resonant frequencies during the propagation of electromagnetic waves through them [66–67]. A structure or image is chiral if its mirror image differs from the original. To achieve a negative refractive index, the typical metamaterial needs to have both negative permittivity (e) and permeability (u) at the same time. Experimental evidence has demonstrated that combining artificially manufactured materials with negative permittivity can result in the production of materials having a negative index. On the other hand, the chiral metamaterial gets closer to a simpler method of obtaining negative refraction and consequently negative index. Because of the asymmetry characteristics of the medium, the chiral media respond differently to the incidence right-handed circular (RHC) and left-handed circular (LHC) polarized waves. In the past ten years, the manipulation of electromagnetic waves through chiral metamaterials has emerged as a popular area of study in transmission mode operations. When compared to naturally occurring chiral material like sugar solution, DNA, and proteins, which were employed to create asymmetric transmission, flawless 90° polarization rotators, etc., the electrically thin chiral structure offers a significant advantage. As a result, for practical use, researchers are always searching for an ultrathin, broad-band, extremely efficient, and angularly stable CMM structure. Among the most important uses of CMS is asymmetric transmission (AT). While the same polarized wave is blocked from the other direction, the chiral structure can powerfully convert linearly or circularly polarized waves into their respective cross-polarization in one direction.

Literature Review

The utilization of optical activity, faraday effect, and anisotropic birefringent crystals in traditional techniques to manipulate the conversion of polarization state was associated with several drawbacks, including bulky volume, narrow bandwidth, and a dependent reaction to the incidence angle. The utilization of artificially created, engineered structures known as metasurfaces, which have subwavelength thickness, cheap cost, flexibility, compact size, and ease of manufacture, allows them to circumvent these restrictions. Polarization conversion comes in two flavors. The initial transformation is called cross-polarization, while the second one is called linear to circular polarization transformation, or vice versa. Any kind of conversion of polarization state can occur in transmission or reflection mode. In the reflection mode, the metamaterial's surface reflection causes the polarization to change forms. In cross conversion, for instance, a horizontal wave that strikes a metasurface might, through reflection, become a vertical wave, and vice versa. On the other hand, in the transmission mode, the polarization changes once it crosses the metamaterial's

surface. A variety of metasurface shapes are intended to accomplish polarization conversion across a broad range of frequencies [46]. According to reference [47], a metasurface based on anisotropic unit cells can be used to achieve the crosspolarization conversion in the reflection.
Anisotropic unit cells are defined as having distinct geometric and physical structures along the x- and y-axes. Anisotropy causes the cross-polarization conversion through the metasurface to occur because it reacts to the linearly polarized wave's normal components differently, causing one component to be reflected at 0 degrees (in phase) and the other at 180 degrees (out of phase). Numerous cross-polarizers based on metasurfaces and anisotropic geometry have been reported in the literature [48–53]. Chiral geometries that can rotate the incident wave's plane of polarization also achieve the cross-polarization conversion. Because chirality precludes C2 mirror symmetry, chiral geometry cannot overlap with its mirror copy. Chiral metamaterial can be used to accomplish the cross-polarization conversion in transmission mode. Strong cross coupling between the electric and magnetic fields is the cause of the cross conversion of polarization in the chiral metamaterial. Different metamaterials based designs have proved the ability to obtain the polarization conversion in transmission mode through the use of chiral geometries. Chiral metamaterials display significant asymmetric transmission, which is the structure that passes an electromagnetic wave in one direction while restraining the same wave in the opposite direction, due to the lack of mirror symmetry in the wave propagation direction. As an illustration, suppose that an x- or y-polarized wave travels through CMM in a forward direction, blocking the identical wave from the opposite side. This asymmetric transmission in CMM is caused by the loss of intercoupling between magnetic and electric fields for one type of linearly polarized wave (the CMM behaves like a perfect electric conductor) and the generation of electric and magnetic cross-coupling for another type of linearly polarized wave (the CMM acts as a perfect magnetic conductor) along the same direction. Strong asymmetric transmission is exhibited by several CCM-based structures, as reported in the literature review. As previously mentioned, chiral metamaterial (CMM) exhibits optical features that can be utilized to rotate the direction of linear polarization. In general, CMM has a higher capacity to rotate the plane of polarization than naturally occurring materials. However, finding chiral geometries that can provide strong cross coupling between the electric and magnetic fields is the primary issue in constructing CMMs. This characteristic, which is also known as cross-coupling efficiency, is essential for cross-polarization in the CMM structure. The CMM has demonstrated increased polarization conversion efficiency as a result of magnetic coupling resonance and electric dipole interaction is responsible for the power ratio in the co- and cross-polarized components. For example, reference demonstrates polarization conversion efficiency exceeding 90 degrees, which is attributed to the magnetic dipole's interaction. The following discusses the state of the art for various CMM-based structures to achieve asymmetric polarization conversion over various frequency bands. Broadband asymmetric transmission (AT) is realized in transmission mode as a result of significant electric and magnetic cross coupling that occurs inside the structure (fabry-perot similar resonance effect). Consequently, reports on the three-layer chiral structure that displays the broad-band response as a result of substantial cross-coupling. A unique three-layered CMM with a strong AT effect and an effective broad-band cross-polarization conversion for linearly polarized waves was proposed in reference [song_down]. Furthermore, the fabry-Perot (FP) type resonance effect is responsible for the broad and effective response. A unique three-layered chiral structure with a simultaneous wide-band of 12.2 GHz (from 4.6 GHz to 16.8 GHz) with high magnitude and a flawless 90° rotator at multiband with reduced dispersion losses. The chirality nature of the x- and y-polarized, or the absence of C2 symmetry in the propagation direction, accounts for the variation in AT

response. Presented chiral multi-layer structure in [82] to demonstrate broad-band AT response with magnitude greater than 0.8 in the infrared range, from 100 THz to 285 THz. The Fabry-Perot resonance effect is responsible for this broadband response. Tri-layered was proposed in 2017. In the microwave frequency, compound chiral metamaterials (CCMM) enable effective polarization conversion and broadband AT. The results of the simulation and testing indicate that the AT effect is larger than 0.8 and the PCR value is greater than 90% in the 4.36 GHz to 14.91 GHz frequency range. This extremely effective design's application is only restricted by the angular instability of the incidence angle. In order to achieve AT with high transmission efficiency of power and amplitude of 90% and 95%, respectively, in the infrared range, a tri-layered chiral structure was proposed in 2018. Additionally, the design can be adjusted to change the operational bandwidth to a different range in the infrared spectrum. The chiral structure of a tri-layered device with two L-shaped resonators etched on both sides of the substrate is introduced in Reference 2014. The proposed design exhibits a wide-band AT effect in the near-infrared region for linearly polarized materials with a maximum magnitude of 0.9. In order to achieve a very wide-band of AT for incidence linearly polarized waves and approximately 90° rotation of polarization in the optical domain, a three-dimensional CMM was proposed in 2018. According to simulation results, only for normal incidence of angle could the reported design provide wide-band AT from 124 THz to 244 THz with amplitude greater than 0.8. These devices all accomplish good polarization conversion and wide band AT responsiveness (in the infrared and microwave bands), but they have three key drawbacks. First off, they were only successful at standard incidence angles. Second, simply a simulation tool is used to obtain the replies. Last but not least, compared to two-layer design, the production of three-layer CMM is more difficult and expensive. From the perspective of a practical application, angular stability is crucial. In answer to this issue, Stephen and colleagues in 2018 presented and described an incredibly thin, bi-layered CMM that produced a wide-band AT response for linearly polarized electromagnetic waves in the microwave range. The suggested chiral structure's experimental and numerical results demonstrate a wide 1.15GHz bandwidth and a high conversion efficiency (>90%). Additionally, the structure response stabilizes at incoming wave angles up to 30 degrees. Figure 2.2 shows the asymmetric response against varying incidence angles. This CCM structure has a further advantage over non-angular chiral structures as it is the first to exhibit angularly stable response up to 30 degrees. This CCM structure has a further advantage over non-angular chiral structures as it is the first to exhibit angularly stable response up to 30°. The only way to increase the angular stability of the AT response is to use active chiral metamaterial. By employing CMM with active pin diode components, the AT effect of EM waves is shown in [88] to be insensitive to the incidence wave angle up to 70°. In order to create wide-band AT of linear EM wave in microwave frequencies (from 10.1GHz to 15GHz) with magnitude (>0.7) and attained PCR value (>92%), the author presented a novel bi-layered chiral structure in 2019. Because of this, two modified resonators are printed on the FR-4 dielectric substrate's two sides. There is good agreement between the results of the simulation and the experiment. Only the broad band response to the usual incident angle is displayed in the suggested design. A twist split ring resonator (TSRR) with 90o rotation on both sides of the dielectric substrate was proposed in 2013 as a polarization transformer for linearly polarized waves. The suggested design exhibits a very low AT value of 0.6 at a single microwave frequency but a high PCR efficiency of 95%. The incidence wave angle affects the single frequency response. In reference, discontinuous bi-layered cross wire strips were examined in order to achieve the AT effect for waves with a normal incidence. At a frequency of 7.64 GHz, the suggested design displays an AT efficiency of 87%. Two layered CMMs were proposed in 2016 to accomplish

wideband AT response for linear EM waves in two opposing directions. The simulation results show that the reported design achieved a maximum magnitude of 0.94 at frequency 11.3GHz and wideband cross-polarization conversion with efficiency (>80%) from 10.27 GHz to 11.57 GHz. However, the AT response value only rises above 0.6, reaching a maximum peak of 0.8 within the designated operating region. In response to the oblique incidence angle, the response is unstable. The maximum value of the AT effect for a type of two-layered examined in 2012 for normal incidence of angle at frequency 10.2 GHz is 0.64. A square metallic hole chiral resonator was proposed in 2017 to demonstrate an efficient and wide band of the AT near-infrared region. With only normal incidence of angle, the suggested design was able to obtain very high AT effect and effective cross-polarization. Dynamic CMM architecture was proposed in 2014 [95] to implement AT for linear EM wave. A square resonator with a tiny gap is printed on both sides of the FR-4 dielectric substrate to form the CMM unit cell. Only at a normal angle of incidence, the proposed design exhibits an AT value of 0.767 and a transmission coefficient magnitude of 0.86 at a frequency of 4.42GHz.

In provided experimental and numerical evidence of the AT and polarization conversion phenomena for linearly polarized waves. The suggested structure achieves PCR 97% and AT value 0.57 at frequency 9.8GHz by using a circular resonator with a tiny gap etched on both sides of the FR-4 substrate. As a result, the suggested design is limited in its response to a single frequency and unstable at oblique angles. A suggested ultra-thin CMM from 2011 obtained the AT response at a single frequency of 6.2GHz by using a U-shaped configuration of four split ring resonators. Furthermore, for four polarization angles of incidence, the proposed structure accomplished symmetric transmission; otherwise, the response is asymmetric. In order to achieve wideband gigantic AT for both linear and circular polarized waves, researchers in 2015 examined metallic chiral meta structures made up of two-layered rotational bars. Only at normal incidence angles was the wide AT response from 250–300 THz obtained by the stated design. Two stacked CMMs demonstrating the AT effect for linearly polarized waves at two distinct frequency bands were presented in 2014. The design achieved AT values of 0.73 and 0.8, and cross transmission coefficient values of 0.88 and 0.92 at frequencies of 5.68 GHz and 10.7 GHz, respectively, according to the findings of the measurement and modeling. The response remains steady when the angle is only normal. In order to provide double broadband AT operation and cross-polarization transformation for the linearly polarized wave, introduced a bi-layered modified CMM in 2019. The two meander-shaped, rotating metallic layers that make up the unit cell of the proposed CMM are arranged on both sides of the incredibly thin FR-4 substrate. Additionally, spanning both frequency bands (8-12 GHz and 14-15 GHz), PCR values larger than 86% and AT response magnitudes smaller than 0.7 were attained. The only steady response angle was the normal incidence angle. Presented in 2014, the bi-layered CMM exhibits dual band AT for plane polarization wave and is made up of two T-shaped coupled resonators. The suggested configuration only displays the AT peak value over two frequency ranges when the incidence angle is normal. The primary drawback of the aforementioned designs is that while they all provide dual band AT responses, the responses are only stable at typical incidence angles.

Methodology

A metal-dielectric-metal structure is used. The schematic top and side views of the proposed chiral metamaterial (CMM) is shown in figure 1. The unit cell of the proposed structure is a simple 'EI' shape resonator printed on two opposite sides of dielectric substrate. The front and back

layers' metal pattern is the same, except that the back-layer's pattern twisted at 90 degree to destroy mirror symmetry in the propagation direction.

Design Steps

By Using the CST, various designing steps and methods are carefully utilized to achieve the desired results in the front, back and 3D view of the unit cell.

Parametric Analysis

For achieving the desired results, adding various slots and cuts in the front side view of the metallic copper. Slots and cuts sizes may varies and step by step analyzing to optimize the desired output. Gaps between slots are varies and carefully adds more slots and cuts to finalizing the desired shape.

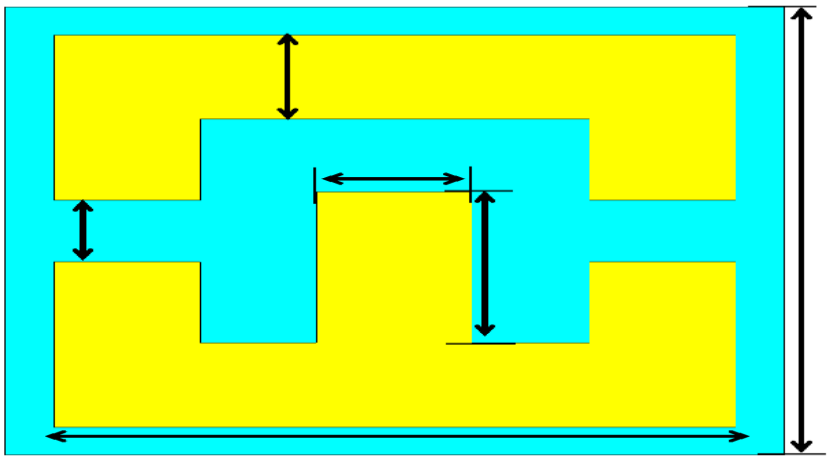

(a) Front metallic side

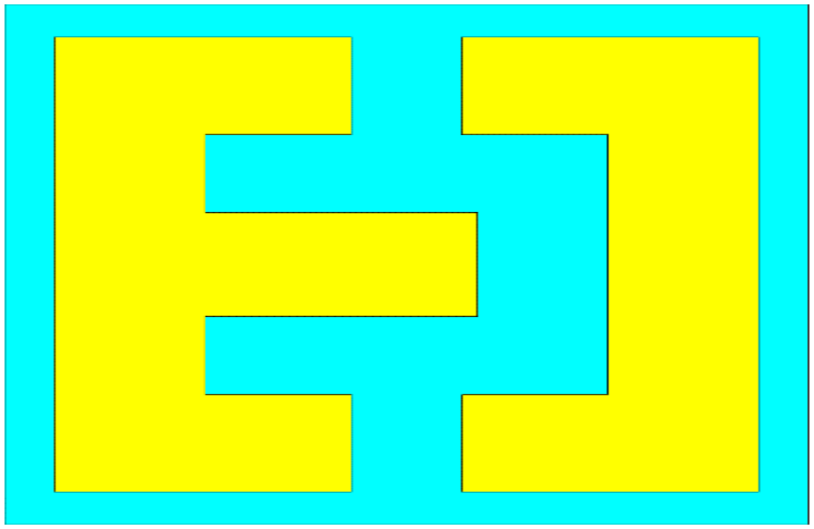

(b) Bottom metallic side

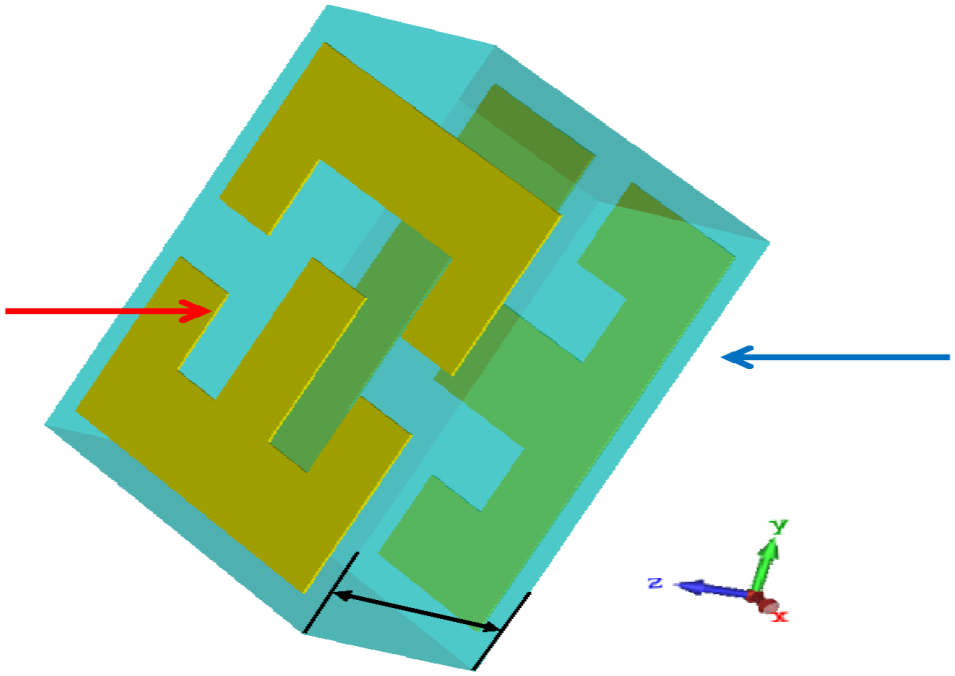

(c) 3-D view of the unit cell.

Fig. 1: Schematic view of unit cell of the suggested CMM: (a) Front metallic side, (b) Bottom metallic side and (c) 3-D view of the unit cell.

Results and Discussions

The simulation results of complex transmission coefficients for linearly polarized waves in the forward (+z) and backward (-z) direction of propagation are depicted in fig. 2(a) and fig. 2(b) respectively. It is seen that the cross-polarization components of transmission spectra show wide, strong peaks. As illustrated in fig. 2(a), for forward direction of propagation, the cross-polarization component Txy exhibits a wide-band response with magnitude more than 0.9 from (14.4-19.5) GHz frequency region. This passband clearly suggests that the proposed structure has a high degree of polarization conversion. For TE incidence (y-polarization) wave along forward propagation direction, this polarization conversion effect is seen over a large bandwidth of 5.1 GHz which is a substantial improvement over prior designs. However, in the same propagation direction, for x-polarized (TM incidence) waves, the structure acts as a mirror reflecting the majority of waves and keeping the magnitude of Tyx less than 0.03 in the same operating bandwidth. This is because the incidence x-polarized wave does not experience cross-coupling. This significant difference in cross-polarization components demonstrates the strong asymmetric transmission (AT) nature of the suggested design for linearly polarized waves. Another crucial information observed from Fig. 2 is that the value of co-polarization coefficients (Tyy and Txx) are equal and remain below 0.16 across the whole frequency range. According to the previous theoretical analysis, it is observed that the identical value of Txx and Tyy guarantees zero AT for incidence circular polarized waves, hence the design has AT only for linear polarization.

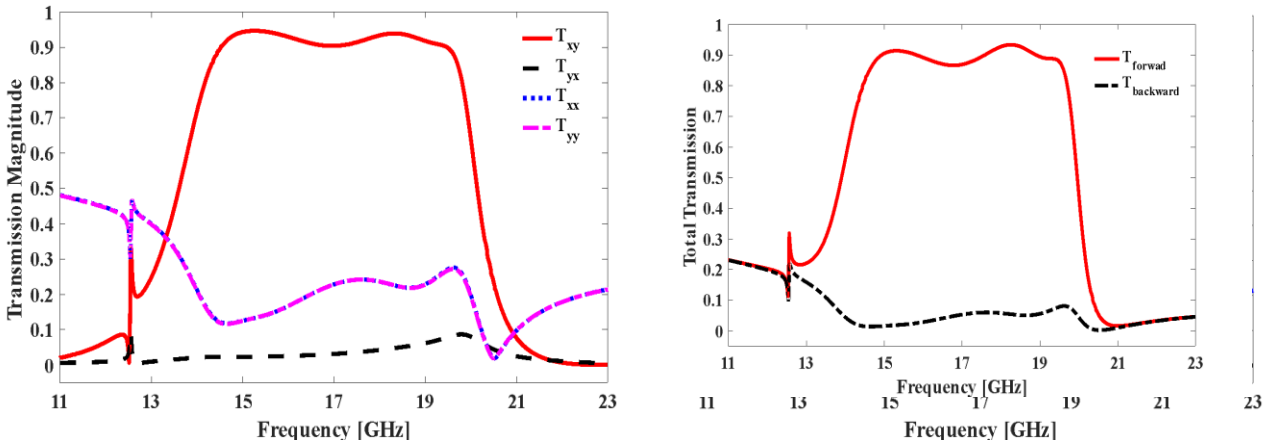

Fig. 2: The linear polarized wave transmission magnitude along the (a) frontward and (b) backward propagation direction.

Furthermore, it can be seen in fig. 2(a) and fig. 2(b) that for backward propagation direction, the cross-polarization components magnitude are interchanged, indicating that the structure will function as a polarization rotator for x-polarized wave when it is impinged from the backside.

Asymmetric Transmission and Total Transmission

In order to measure the AT response of the suggested design, the AT parameter Δ has been calculated from the transmission coefficients using equation (1). The magnitude of the AT parameters Δ for incident x- and y-polarized waves are shown in Fig. 3(a). It is observed that the suggested design exhibits strong AT for linearly polarized waves having magnitude greater than 0.8 over wide frequency range (14.48 GHz to 19.51 GHz) and getting their maximum magnitude of 0.92. Additionally, it can be shown in fig. 3(a) that the peaks for and are located oppositely. The presence of contrary peaks for and implies that in the forward propagation direction, one polarization (TE) is permitted whereas the other polarization (TM) is prohibited, and this situation is reversing in the backward propagation direction. It is observed that when compared with investigated studies, the suggested single dielectric layer structure demonstrates a broad-band, high magnitude of Δ at microwave range of frequencies.

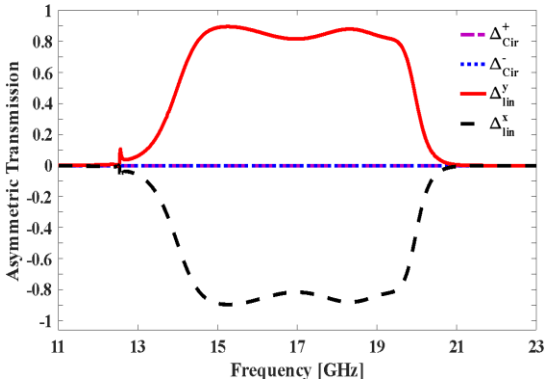

Fig. 3: (a) The asymmetric transmission Δ for y- and x- linearly polarized waves and (b) the total transmission for y-polarized waves in forward and backward directions.

The strong AT behavior of the proposed design is further validated by total transmission results, which is computed from the cross- and co-polarized components as described in equation (?). Figure 4.3(b) depicts the total EM transmission for a y-polarized wave in the forward (-z) and backward (+z) propagation of direction. Because of the significant difference in cross polarization components, the total transmission from both directions for forward and backward excitations is completely different. In forward direction of propagation, the total transmission spectra for y-polarized waves show amplitude greater than 0.8 with a maximum transmission value of 0.92 in the effective operating bandwidth. However, in the backward direction, it shows an amplitude less than 0.15.

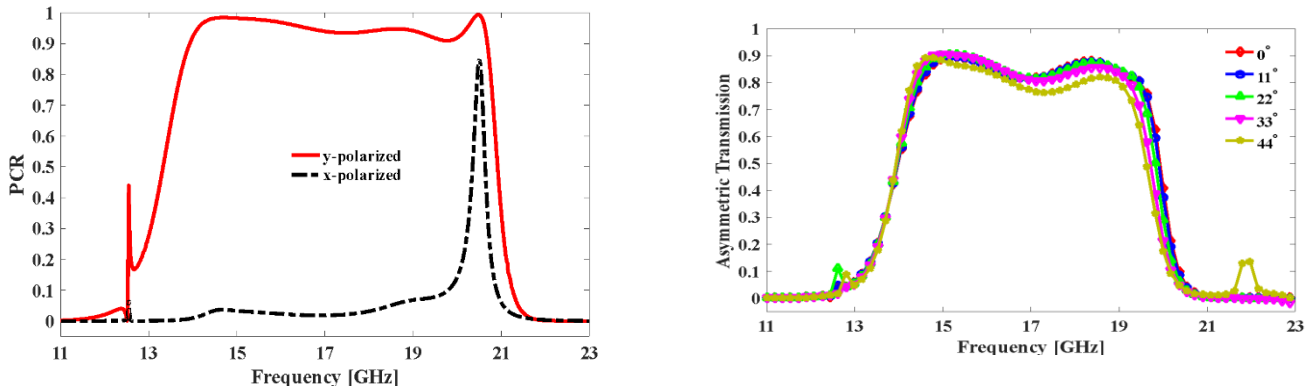

Fig. 4: (a) Simulation results of PCR for linearly polarized waves in forward direction. (b) Asymmetric transmission for different incidence angles.

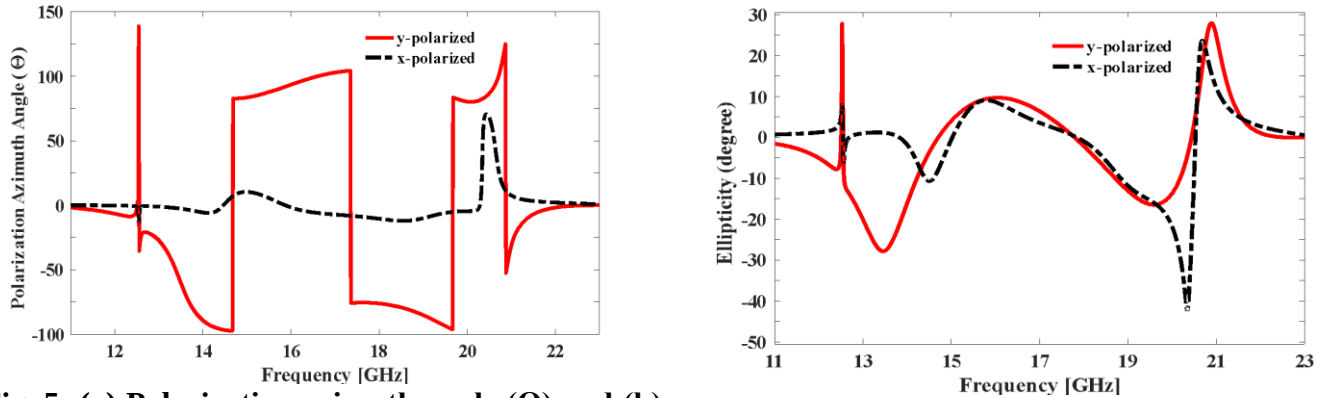

Fig. 5: (a) Polarization azimuth angle (Θ) and (b) ellipticity (η) for x- and y- linearly polarized wave along in forward direction.

By demonstrating the mechanism of cross-coupling between the electric and magnetic fields, the physics underlying the AT phenomena can be better understood. The induced surface current distribution at 14.5 GHz resonance frequency, caused by a y-polarized wave propagating forward

through CMM, is shown in Figure 6. Depending on the geometry of the structure, a pair of symmetric and anti-symmetric electric currents between the upper and bottom layers of CMM are formed when the impinging wave on the slab of CMM is linearly polarized. These currents result in the induction of an electric and magnetic dipole, respectively. Figures 1(a) and 1(b) make it abundantly evident that there are two sets of parallel current and three sets of antiparallel current between the top and bottom layers of the CMM.

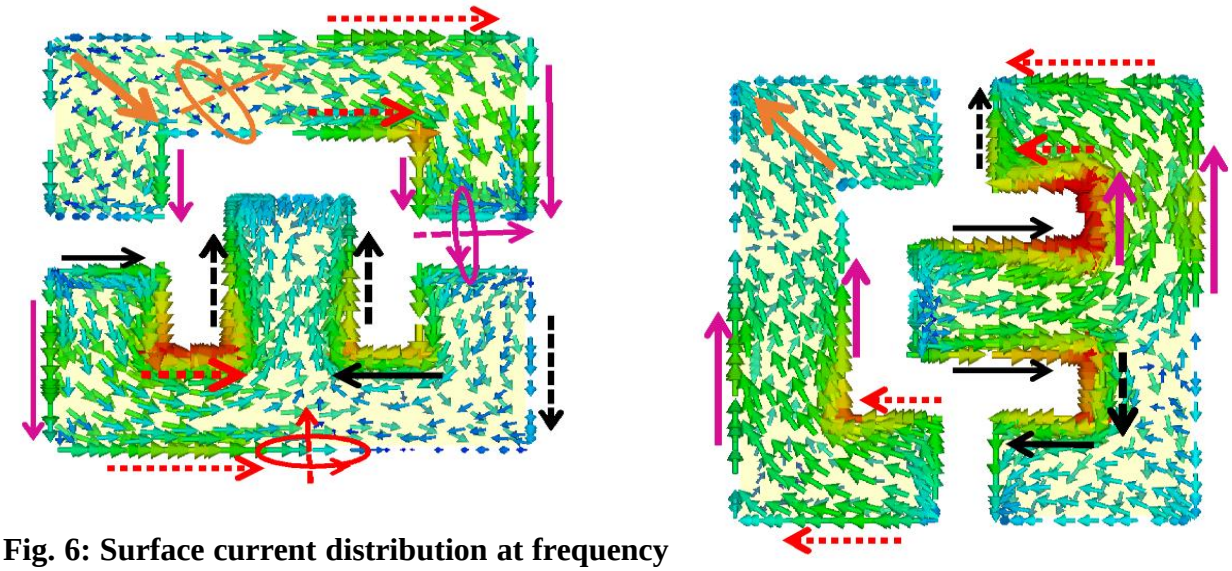

Fig. 6: Surface current distribution at frequency of 14.8 GHz for incidence y-polarized wave (a) upper metallic layer and (b) bottom metallic layer of the suggested structure.

Figure 6 clearly shows the current distribution frequency at 14.8 GHz for the front and back sideview of the proposed structure. The magnetic moment m1, m2, and m3 produced by the anti-symmetric current flowing in the opposite direction induces H1, H2, and H3 in turn, which breaks down into x- and y-components. The components of H1, H2, and H3 that are parallel to the incidence field (E_{inc}) are cross-coupled, which results in a cross-polarization transformation, since the incidence field is along the y-direction (for TE-polarized EM wave). On the other hand, the parts of H1, H2, and H3 that are perpendicular to the incidence field never take part in the conversion of polarization. Similarly, along the x- and y-axes, the two sets of symmetric current producing electric dipoles, p1 and p2, will generate the electric field, E1 and E2, respectively. In the polarization conversion from y-to-x transformation, the E1 and E2 components that are parallel to the applied incidence field will never be involved. Despite the fact that the elements of E1 and E2 that are orthogonal to the incidence field have a significant cross-coupling, this has the effect of rotating cross-polarization.

Conclusion

To sum up, we have developed and created an ultrathin chiral metamaterial (CMM) that may be used to manipulate and control the polarization state of electromagnetic waves across a microwave frequency range. In the first proposed design, a novel two-layered CMM is created to achieve wideband asymmetric transmission for incidence linearly polarized waves with excellent polarization conversion efficiency. The two basic, electrically thin V-shaped resonators that are printed on both sides of the Roger 5080 dielectric substrate make up the CMM. The suggested

design produced a broad AT response bandwidth of 1.68 GHz with a magnitude more than 0.9 for linear polarization and concurrently a crosspolarization conversion efficiency (>92%) spanning the 8.48–10.16 GHz frequency range. Additionally, over the specified operating frequency band, the device exhibits stability against variations in the incoming wave angle up to 45 degrees while maintaining a broadband AT response with magnitudes greater than 0.8. In the second design, a novel bi-layered CMM structure is designed to significantly boost the operational AT bandwidth and crosspolarization conversion. A few EI-shaped resonators printed on both sides of the Roger 5080 substrate make up the CMM design. Excellent wideband AT phenomenon is achieved for both normal incidence and oblique angle up to 33°, with magnitude higher than 0.8 from 14.48 GHz to 19.51 GHz (bandwidth of 5.03 GHz). Moreover, over the working frequency range, the polarization conversion ratio is larger than 85%.

References

(1) H. T. Chen, A. J. Taylor, and N. Yu, "A review of metasurfaces: Physics and applications," *Reports Prog. Phys.*, vol. 79, no. 7, 2016.

(2) E. Plum *et al.*, "Metamaterial with negative index due to chirality," *Phys. Rev. B - Condens. Matter Mater. Phys.*, vol. 79, no. 3, pp. 1–6, 2009.

(3) M. I. Khan and F. A. Tahir, "An angularly stable dual-broadband anisotropic cross polarization conversion metasurface," *J. Appl. Phys.*, vol. 122, no. 5, p. 53103, 2017.

(4) O. Access, "Chiral metamaterials : enhancement and control of optical activity and circular dichroism," 2015.

(5) Hailin Cao et al, "90° Polarization Rotator Using a Bilayered Chiral Metamaterial," *Appl. Phys. Lett.*, vol. 96, no. 20, pp. 1–10, 2010.

(6) L. Stephen, N. Yogesh, V. Subramanian, L. Stephen, N. Yogesh, and V. Subramanian, "Broadband asymmetric transmission of linearly polarized electromagnetic waves based on chiral metamaterial," vol. 33103, 2018.

(7) M. Mutlu, Z. Li, and E. Ozbay, "Chiral metamaterials: From negative index to asymmetric transmission," *2013 7th Eur. Conf. Antennas Propagation, EuCAP 2013*, no. Eucap, pp. 3687–3688, 2013.

(8) V. A. Fedotov, P. L. Mladyonov, S. L. Prosvirnin, A. V Rogacheva, Y. Chen, and N. I. Zheludev, "Asymmetric Propagation of Electromagnetic Waves through a Planar Chiral Structure," vol. 167401, no. October, pp. 1–4, 2006.

(9) S. O. Material, I. S. I. Web, S. This, H. Press, N. York, and A. Nw, "A Chiral Route to Negative Refraction," vol. 1353, no. 2004, 2012.

(10) "Journal of Electromagnetic Waves and Applications Waves and Energy in Chiral Nihility," no. March 2013, pp. 37–41, 2012.

(11) J. K. Gansel, M. Latzel, A. Frölich, J. Kaschke, M. Thiel, and M. Wegener, "Tapered gold-helix metamaterials as improved circular polarizers," *Appl. Phys. Lett.*, vol. 100, no. 10, pp. 2010–2013, 2012.

(12) J. K. Gansel *et al.*, "Gold helix photonic metamaterial as broadband circular polarizer," *Science (80-.).*, vol. 325, no. 5947, pp. 1513–1515, 2009.

(13) M. Decker, M. W. Klein, M. Wegener, and S. Linden, "Circular dichroism of planar chiral magnetic metamaterials," *Opt. Lett.*, vol. 32, no. 7, p. 856, 2007.

(14) J. Zhou, J. Dong, B. Wang, T. Koschny, M. Kafesaki, and C. M. Soukoulis, "Negative refractive index due to chirality," *Phys. Rev. B - Condens. Matter Mater. Phys.*, vol. 79, no. 12, pp. 3–6, 2009.

(15) X. Xiong *et al.*, "Construction of a chiral metamaterial with a U-shaped resonator assembly," *Phys. Rev. B - Condens. Matter Mater. Phys.*, vol. 81, no. 7, pp. 1–6, 2010.
(16) X. Ma, C. Huang, M. Pu, C. Hu, Q. Feng, and X. Luo, "Multi-band circular polarizer using planar spiral metamaterial structure," *Opt. Express*, vol. 20, no. 14, p. 16050, 2012.
(17) Y. Cui, L. Kang, S. Lan, S. Rodrigues, and W. Cai, "Giant Chiral Optical Response from a Twisted-Arc Metamaterial," vol. 200, no. 6, pp. 1–7, 2014.
(18) A. E. Serebryannikov, "One-way diffraction effects in photonic crystal gratings made of isotropic materials," no. October, pp. 1–13, 2009.
(19) Z. Wang, Y. Chong, J. D. Joannopoulos, and M. Soljac, "Observation of unidirectional backscattering-immune topological electromagnetic states," vol. 461, no. October, 2009.
(20) S. Cakmakyapan *et al.*, "Experimental validation of strong directional selectivity in nonsymmetric metallic gratings with a subwavelength slit," vol. 51103, no. November 2018, 2017.
(21) L. Fan, "An All-Silicon Passive," vol. 447, no. 2012, 2014.
(22) V. R. Tuz and S. L. Prosvirnin, "Bistability , multistability , and nonreciprocity in a chiral photonic bandgap structure with nonlinear defect," vol. 28, no. 5, pp. 1002–1008, 2011.
(23) C. Genet and L. Bel, "Reciprocity and optical chirality," vol. 2, no. 1, pp. 1–20, 2015.
(24) Y. Cheng, Y. Nie, X. Wang, and R. Gong, "An ultrathin transparent metamaterial polarization transformer based on a twist-split-ring resonator," Appl. Phys. A Mater. Sci. Process., vol. 111, no. 1, pp. 209–215, 2013.
(25) C. Huang, Y. Feng, J. Zhao, Z. Wang, and T. Jiang, "Asymmetric electromagnetic wave transmission of linear polarization via polarization conversion through chiral metamaterial structures," vol. 195131, pp. 1–5, 2012.
(26) T. Pertsch and F. Lederer, "Asymmetric Transmission of Linearly Polarized Light at Optical Metamaterials," vol. 253902, no. June, pp. 1–4, 2010.
(27) Z. Li et al., "Broadband diodelike asymmetric transmission of linearly polarized light in ultrathin hybrid metamaterial," vol. 201103, no. November 2018, 2017.
(28) M. Mutlu, A. E. Akosman, A. E. Serebryannikov, and E. Ozbay, "Asymmetric chiral metamaterial circular polarizer based on four U-shaped split ring resonators," vol. 36, no. 9, pp. 1653–1655, 2011.
(29) Z. Li, M. Mutlu, and E. Ozbay, "Highly asymmetric transmission of linearly polarized waves realized with a multilayered structure including chiral metamaterials," vol. 75107.
(30) M. Kang, J. Chen, H. Cui, Y. Li, and H. Wang, "Asymmetric transmission for linearly polarized electromagnetic radiation Abstract :," vol. 19, no. 9, pp. 8347–8356, 2011.
(31) D. Liu, Z. Xiao, X. Ma, Q. Ma, X. Xu, and Z. Wang, "Asymmetric transmission of chiral metamaterial slab with double L resonators," Opt. Commun., vol. 338, pp. 359–365, 2015.
(32) F. Dincer et al, "Asymmetric transmission of linearly polarized Waves and Dynamically Wave Rotation," vol. 140, no. May, pp. 227–239, 2013.
(33) K. Chen, Y. Feng, L. Cui, J. Zhao, T. Jiang, and B. Zhu, "Dynamic control of asymmetric electromagnetic wave transmission by active chiral metamaterial," Sci. Rep., vol. 7, no. January, pp. 1–10, 2017.
(34) X.Huang, D.Yang, S.Yu, L.Guo, Lin.Guo, H.Yang"Dual-band asymmetric transmission of linearly polariz using Π-shaped metamaterial." Appl. Phys. B Lasers Opt., vol. 170, no 23 pp. 409–411, 2014.

(35) Z. Zhou and H. Yang, “Triple-band asymmetric transmission of linear polarization with deformed S-shape bilayer chiral metamaterial,” Appl. Phys. A Mater. Sci. Process., vol. 119, no. 1, pp. 115–119, 2015.
(36) X. Li, R. Feng, and W. Ding, “Extremely high contrast asymmetric transmission with linear tunability in chiral metamaterials,” J. Phys. D. Appl. Phys., vol. 51, no. 14, pp. 0–6, 2018.
(37) F. Mirzamohammadi, J. Nourinia, C. Ghobadi, and M. Majidzadeh, “A bi-layered chiral metamaterial with high-performance broadband asymmetric transmission of linearly polarized wave,” AEU - Int. J. Electron. Commun., vol. 98, pp. 58–67, 2018.
(38) J. Shi et al., “Dual-band asymmetric transmission of linear polarization in bilayered chiral metamaterial,” Appl. Phys. Lett., vol. 102, no. 19, 2013.
(39) L. Wu, M. Zhang, B. Zhu, J. Zhao, T. Jiang, and Y. Feng, “Dual-band asymmetric electromagnetic wave transmission for dual polarizations in chiral metamaterial structure,” Appl. Phys. B Lasers Opt., vol. 117, no. 2, pp. 527–531, 2014.
(40) K. K. Xu, Z. Y. Xiao, J. Y. Tang, D. J. Liu, and Z. H. Wang, “Ultra-broad band and dualband highly efficient polarization conversion based on the three-layered chiral structure,” Phys. E Low-Dimensional Syst. Nanostructures, vol. 81, pp. 169–176, 2016.
(41) D. J. Liu, Z. Y. Xiao, X. L. Ma, and Z. H. Wang, “Broadband asymmetric transmission and multi-band 90° polarization rotator of linearly polarized wave based on multi-layered metamaterial,” Opt. Commun., vol. 354, pp. 272–276, 2015.
(42) “Journal of Electromagnetic Waves and Applications Waves and Energy in Chiral Nihility,” no. March 2013, pp. 37–41, 2012
(43) J. K. Gansel, M. Latzel, A. Frölich, J. Kaschke, M. Thiel, and M. Wegener, “Tapered gold-helix metamaterials as improved circular polarizers,” Appl. Phys. Lett., vol. 100, no. 10, pp. 2010–2013, 2012.
(44) J. K. Gansel et al., “Gold helix photonic metamaterial as broadband circular polarizer,” Science (80-.)., vol. 325, no. 5947, pp. 1513–1515, 2009.
(45) C. Huang, Y. Feng, J. Zhao, Z. Wang, and T. Jiang, “Asymmetric electromagnetic wave transmission of linear polarization via polarization conversion through chiral metamaterial structures,” vol. 195131, pp. 1–5, 2012.
(46) T. Pertsch and F. Lederer, “Asymmetric Transmission of Linearly Polarized Light at Optical Metamaterials,” vol. 253902, no. June, pp. 1–4, 2010.
(47) Z. Li et al., “Broadband diodelike asymmetric transmission of linearly polarized light in ultrathin hybrid metamaterial,” vol. 201103, no. November 2018, 2017.
(48) M. Mutlu, A. E. Akosman, A. E. Serebryannikov, and E. Ozbay, “Asymmetric chiral metamaterial circular polarizer based on four U-shaped split ring resonators,” vol. 36, no. 9, pp. 1653–1655, 2011.
(49) Z. Li, M. Mutlu, and E. Ozbay, “Highly asymmetric transmission of linearly polarized waves realized with a multilayered structure including chiral metamaterials,” vol. 75107.
(50) M. Kang, J. Chen, H. Cui, Y. Li, and H. Wang, “Asymmetric transmission for linearly polarized electromagnetic radiation Abstract :,” vol. 19, no. 9, pp. 8347–8356, 2017.
(51) L. Wu, M. Zhang, B. Zhu, J. Zhao, T. Jiang, and Y. Feng, “Dual-band asymmetric electromagnetic wave transmission for dual polarizations in chiral metamaterial structure,” Appl. Phys. B Lasers Opt., vol. 117, no. 2, pp. 527–531, 2018.
(52) K. K. Xu, Z. Y. Xiao, J. Y. Tang, D. J. Liu, and Z. H. Wang, “Ultra-broad band and dualband highly efficient polarization conversion based on the three-layered chiral structure,” Phys. E Low-Dimensional Syst. Nanostructures, vol. 81, pp. 169–176, 2019.

(53) D. J. Liu, Z. Y. Xiao, X. L. Ma, and Z. H. Wang, “Broadband asymmetric transmission and multi-band 90° polarization rotator of linearly polarized wave based on multi-layered metamaterial,” Opt. Commun., vol. 354, pp. 272–276, 2019.